Study of dynamic processes on semiconductor surfaces using time-resolved scanning tunneling microscopy

2010 J. Phys.: Condens. Matter 22 264007

(http://iopscience.iop.org/0953-8984/22/26/264007)

J. Phys.: Condens. Matter **22** (2010) 264007 (6pp) doi:10.1088/0953-8984/22/26/264007

Study of dynamic processes on semiconductor surfaces using time-resolved scanning tunneling microscopy

Amirmehdi Saedi, Bene Poelsema and Harold J W Zandvliet[1]

Physical Aspects of Nanoelectronics and Solid State Physics, MESA$^+$ Institute for Nanotechnology, University of Twente, PO Box 217, 7500 AE Enschede, The Netherlands

E-mail: h.j.w.zandvliet@tnw.utwente.nl

Received 11 January 2010, in final form 13 February 2010
Published 14 June 2010
Online at stacks.iop.org/JPhysCM/22/264007

Abstract
The time resolution of a conventional scanning tunneling microscope can be improved by many orders of magnitude by recording open feedback loop current–time traces. The enhanced time resolution comes, however, at the expense of the ability to obtain spatial information. In this paper, we first consider the Ge(111)-c(2 × 8) surface as an example of how surface dynamics can show up in conventional STM images. After a brief introduction to the time-resolved scanning tunneling microscopy technique, its capabilities will be demonstrated by addressing the dynamics of a dimer pair of a Pt modified Ge(001).

(Some figures in this article are in colour only in the electronic version)

1. Introduction

Understanding the dynamics of surfaces is important from a scientific as well as a technological perspective. Surface dynamics plays a key role in reactivity and mass transport processes, which accordingly affects the functionality and stability of small structures and devices. The latter is even more relevant for structures and devices in the nanometer range, where the surface to volume ratio is large. Many surface science techniques provide information on dynamic phenomena at surfaces, but only a few of them have sufficient spatial resolution to give detailed information on the atomic processes that underlie these dynamic processes. While field ion microscopy (FIM) is limited to the study of the dynamics of atoms at the apex of sharp metallic tips [1], scanning tunneling microscopy (STM) allows one to study basically any semiconductor or metal surface, making it an ideal instrument for studying surface dynamical processes [2]. One important problem associated with STM is, however, its rather poor temporal resolution. Despite this severe drawback STM has been used to study several dynamical surface processes, such as atom and dimer diffusion [3, 4] and thermal step fluctuations [5, 6].

For a conventional STM, the time required to record a single image is of the order of 1 min. This translates into a frame rate of only 0.01 Hz, which is insufficient for studying many dynamic processes. Recently different groups have tried to enhance the temporal resolution of the STM by redesigning its mechanical and electronic parts, enabling it to reach frame rates up to ∼1–100 Hz [7, 8]. However, this is still far slower than many dynamic processes, which can occur on timescales as small as picoseconds. A simple way to overcome this deficiency is time-resolved scanning tunneling microscopy (TR-STM). As will be shown this technique can improve the time resolution of a conventional STM up to seven orders of magnitude.

This paper is divided into three main sections. First we will discuss how surface dynamics can show up in conventional STM images. As an example, we will consider a Ge(111)-c(2 × 8) surface that is lightly dosed with platinum. In section 3 the technique TR-STM will be introduced. It will be shown how this method can provide a deeper insight into the dynamics of the adatoms of Ge(111). In section 4 TR-STM will be used to its full potential to study a more complex system, namely the Pt modified Ge(001) surface.

[1] Author to whom any correspondence should be addressed.

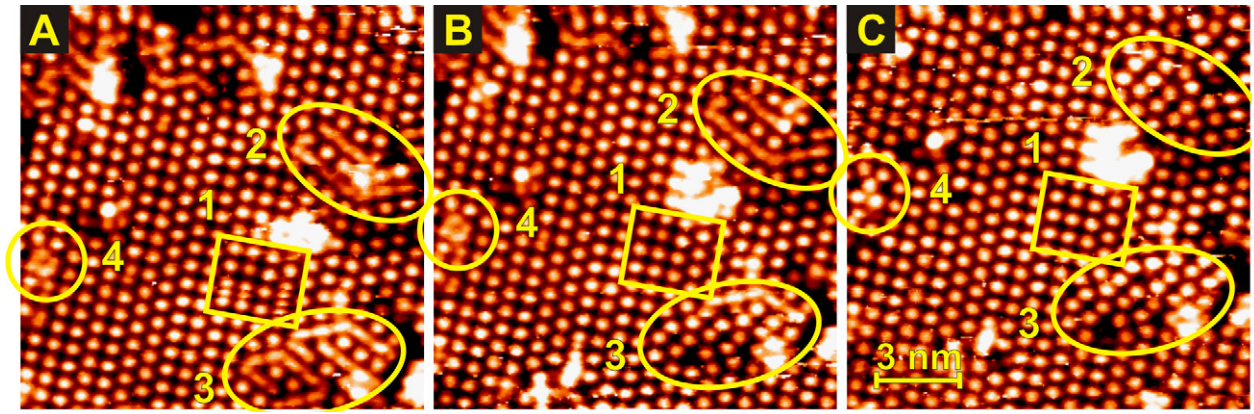

Figure 1. A sequence of images of Ge(111) recorded with a conventional STM at room temperature. Time lapse between the images is 2 min (sample voltage is 2.0 V and tunnel current is 0.5 nA). The images show different dynamic processes caused by mobile Ge adatoms. The hopping frequency of the adatoms outlined by ellipses, is beyond the frame rate of the STM.

2. Dynamics of Ge(111)-c(2 × 8)

The Ge(111) surface exhibits a c(2 × 8) reconstruction that is comprised of (2×2) and c(4×2) building blocks [9–18]. These building blocks consist of Ge adatoms that reside in so-called T_4 positions. These adatoms have a three-fold coordination with respect to the underlying lattice. Since the adatom layer is equivalent to a 1/4 monolayer, not all atoms of the underlying lattice are coordinated to an adatom. A 1/4 monolayer of so-called rest atoms are not involved in the bonding with the adatom layer. These rest atoms have a saturated dangling bond and can therefore be imaged at negative sample biases. The adatoms, on the other hand, have an empty dangling bond and can therefore be imaged best at positive sample biases.

Since there exist in principle three equivalent rotational c(2 × 8) domains, the Ge(111) surface contains a network of phase boundaries that separate different c(2 × 8) domains from each other. The adatom reconstructed Ge(111) exhibits the largest disorder in regions in the direct vicinity of these phase boundaries.

The adatoms of the Ge(111) are rather mobile, even at room temperature, and therefore this system is an ideal system to study with STM. Different possible mechanisms for adatom diffusion on Ge(111) have been proposed in the literature. Among them are: uncorrelated movement [19], correlated sequential movement [20] and correlated simultaneous movement (concerted movement) of adatoms [21]. Here 'correlated movement' means that a hopping adatom triggers the diffusion of its neighbor adatom.

The samples have been cut from an undoped Ge(111) wafer and cleaned in ultrahigh vacuum by cycles of Ar ion bombardment at 800 eV and annealing at 1150 K. This procedure results in atomically clean and virtually defect free Ge surfaces [22]. After cleaning the Ge(111) surface, ∼2% of a monolayer of Pt was deposited on the substrate by using a homebuilt evaporator. We have deposited the Pt because it will lead to an increase of the number density of vacancies and thus to a more dynamic surface. The sample was subsequently annealed at 1100 K. After the sample has been cooled down to room temperature it is transferred to the STM for imaging.

Figure 1 shows a sequence of empty states images of the Ge(111) surface recorded at room temperature. The time required to take each frame was 2 min. Although, the c(2 × 8) reconstruction is clearly visible, many defects such as missing adatoms and adatom islands are present. Many of these defects are induced by Pt, since Pt can easily dissolve and penetrate into the Ge crystal, which induces a disordered, vacancy rich, top layer. The regions in the vicinity of defects or phase boundaries are known to be more susceptible for showing dynamics. In the sequence of images shown in figure 1 several rearrangement events can be observed.

In square 1 (figure 1(A)), at least three adatoms show up several times during scanning. This is illustrated by the additional small spots in the $[1\bar{1}0]$ direction that are located in between the regular adatom positions. The latter is consistent with the fact that the diffusion barrier of an adatom in the $[1\bar{1}0]$ direction (parallel to the adatom rows) is lower than in the $[11\bar{2}]$ direction (perpendicular to the adatom rows). By following square 1 in figures 1(B) and (C), one has to conclude that the adatoms do not diffuse in images (B) and (C).

Ellipses 2 and 3 also contain evidence that Ge(111) exhibits dynamics at room temperature. In figure 1(A) some of the adatoms seem to become dim and elongated along $\langle 1\bar{1}0\rangle$ directions leading to a worm like appearance. Close inspection of the images reveals that this appearance is due to fast motion of adatoms between neighboring T_4 sites. This has been done by superimposing a hexagonal grid on the STM images and determining the underlying T_4 site positions [18]. As can be observed, these dynamic events disappear and reappear at random. What eventually remains is (see figure 1(C)) a set of immobile adatoms and a vacancy at one of its ends. Fast diffusion of this vacancy back and forth along the worms is the origin of the worm like appearance. The facts, that (1) all the atoms in the worms have a similar elongated appearance and (2) in subsequent frames they stop moving simultaneously, make it very plausible that this diffusion process is correlated.

The last notable feature in these frames is indicated by label 4. In figure 1(A) the feature seems to consist of four atoms. It has a blurry appearance, which gives rise to a ring like shape. By following this feature in figures 1(B) and (C) one

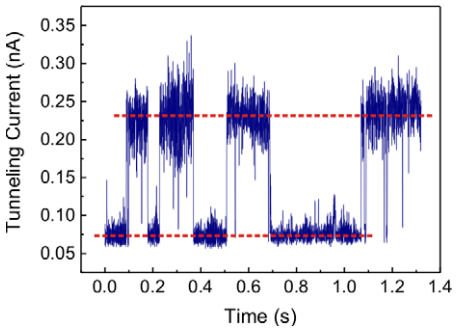

Figure 2. An example of a I–t trace obtained by TR-STM on Ge(111). The tunnel current switches back and forth between two well-defined levels. Each switching event in the tunneling current corresponds to an adatom hopping event in the vicinity of the tip. Sample bias is 2.0 V.

can see that it eventually converts to three stationary adatoms. So the ring like feature is most probably due to a sequence of diffusion events of these three atoms.

3. Time-resolved scanning tunneling microscopy

It is clear that in the above case the hopping frequency of the mobile adatoms exceeds the frame rate of the STM. A way to obtain more temporal information of these processes would be the application of the TR-STM technique [23, 24]. In order to measure the dynamics at a predefined position on the surface, one first has to locate this point, position the tip over the feature of interest, switch off the feedback circuit and then record the current as a function of time. Because the tunneling current decays exponentially with increasing tip–sample separation, even the slightest movement or rearrangement event underneath the tip will result in a jump in the tunneling current.

Using this method the time resolution is limited by the bandwidth of the preamplifier, rather than the frame rate of the STM. The current commercial preamplifiers have bandwidths up to ∼500 kHz, which means that dynamic processes with hopping frequencies up to 100–200 kHz can be studied.

A typical result of a TR-STM measurement recorded near a T_4 site of a Ge(111) surface is shown in figure 2. This graph resembles a telegraphic signal and the current switches back and forth between two well-defined values. The latter corresponds to the diffusion of an adatom between two adjacent T_4 sites. This graph can be used to extract information on the average hopping frequency, the distribution of residence times, etc. From this data one can determine the potential landscape.

In the next section we apply the TR-STM method to study another, more complex example, namely the Pt/Ge(001) system.

4. Dynamics of the Pt modified Ge(001)

It is common knowledge that the deposition of metals on clean semiconductor surfaces can lead to a variety of reconstructions and structures with physical and chemical properties that are often significantly different from the clean semiconductor surfaces. Since metal modified semiconductor surfaces exhibit a myriad of novel properties, these structures offer possibilities for future devices.

One intriguing example is the Pt modified Ge(001) surface. Self-organized Pt nanowires are formed by deposition of a fraction of a monolayer of Pt on clean Ge(001), followed by annealing at 1050–1100 K. The details of the fabrication process and the electronic and structural properties of this structure have been discussed in detail elsewhere [25, 26].

Figure 3(A) shows an STM image of the Pt modified Ge(001) surface at 4.7 K. The atomic configuration of a single nanowire is also illustrated in figure 3(E). The unit cell of these nanowires consists of four atoms forming a pair of dimers, as shown in figure 3(B). At room temperature the dimer bond is aligned parallel to the surface plane, resulting in a 2× periodicity along the nanowire direction. At low temperatures (<80 K) the dimers buckle in an out-of-phase fashion, leading to a 4× periodicity [27]. Preliminary experiments performed

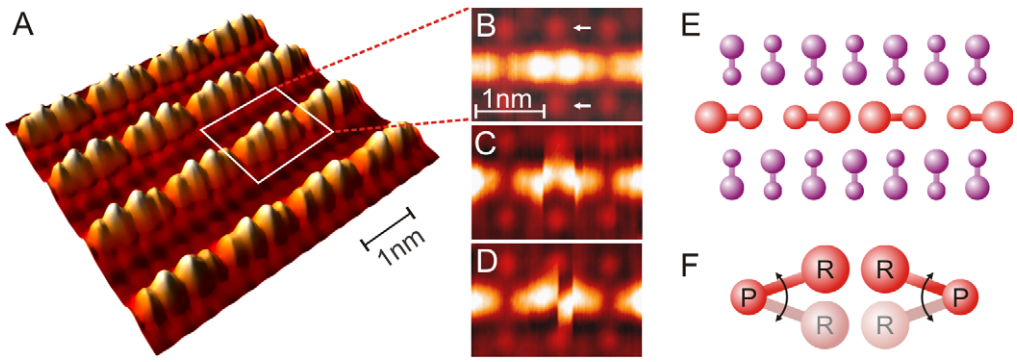

Figure 3. (A) An STM image of atomic chains on Ge(001) at 4.7 K, gap voltage −1.5 V and tunnel current 0.5 nA. Bright protrusions are the atoms that make up the atomic width chains in the image. As a result of a Peierls instability, the chains exhibit a four-fold periodicity with dimers paired together, giving a periodic low–high–high–low appearance of the atoms in the chains. (B) Top view of a regular dimer pair at 77 K, gap voltage −1.0 V and tunneling current 0.8 nA. Two terrace atoms can be seen to protrude from the Ge(001) surface indicated by the white arrows. ((C) and (D)) Two subsequent images of a dimer pair that exhibits mobility. The reconfiguration of the dimer pair is too fast to image and shows up as a discontinuity as the tip is scanned across the chain. (E) Schematic diagram of the dimerized atomic chain and the underlying substrate. (F) A model of the flipping dimers in (C) and (D).

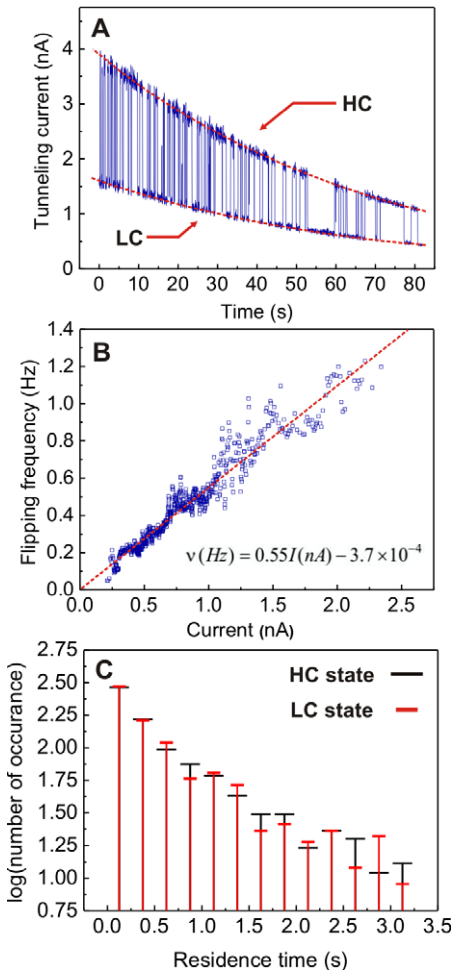

Figure 4. Current–time trace of the APM at 77 K, gap voltage −1.0 V, open feedback loop and initial tunnel current 1.5 nA. (A) The telegraphic signal indicates flipping of the APM between two well-defined states. The decay of current with time is due to drifting of the tip away from the surface. (B) Flipping frequency versus tunnel current. (C) Distribution of residence times of the high current (HC) and low current (LC) states.

in the temperature range from 4.7 to 300 K, have not provided any evidence for any dynamic behavior of these dimers other than the small change in buckling angle. Recently, however, we found that, occasionally, neighboring dimers pairs exhibit a substantial amount of motion [28].

Figures 3(C) and (D) shows the two center atoms of a specific dimer pair rearrange repeatedly. Each discontinuity in the contour is due to a rearrangement event of the dimer pair during scanning. Based on the contours that have been extracted from many STM images, it is clear that only the two center atoms of the dimer pair move, as is illustrated in figure 3(F). These two center atoms move back and forth in the surface plane. We designate the two outer atoms as pivot atoms and the two center atoms are referred to as the revolving atoms. These are marked with (P) and (R), respectively in figure 3(F). The two dimers behave as the flippers of a pinball machine. Therefore we have coined this small atomic structure as an atomic pinball machine (APM).

Since the temporal resolution of an STM is insufficient to study the dynamic behavior of the APM, we have applied the TR-STM technique here. The STM tip was positioned close to the dimer pair, but not at one of its two symmetry axes. The current–time graphs allow us to directly measure the frequency of the switching motion of the dimers. Figure 4(A) shows a typical time trace obtained by this method. Similar to a telegraphic signal, the current switches back and forth between two levels, as indicated by red dashed lines. Each red line corresponds to a specific configuration of the APM. The dashed line with the higher current is indicated by HC in the graph and corresponds to the high current state. Similarly LC stands for the low current state. As can be seen from the graph, the average tunneling current decays with time, indicating that the tip drifts slightly away from the surface during the measurement. This is due to the fact that the feedback loop was switched off and the duration of the measurement was quite long (82 s). In addition, it also seems as if the switching frequency of the APM is considerably higher at the beginning of the measurement as compared to the end of the measurement. This is a first indication that the flipping process of the APM dimers is induced by the tunneling process itself. After analyzing many current time traces we found a linear dependence between switching frequency of the APM and the average tunnel current (figure 4(B)). This linear dependence implies that the dimer flipping event is a single electron process. From the slope of the curve, one extracts an efficiency of 1.1×10^{-9} dimer switching events per tunneling electron. Furthermore, a linear extrapolation of the curve intersects the origin of the graph. The latter means that the flipping dynamics is fully tunneling current induced. The configuration of the pinball machine can thus be altered by simply injecting electrons into the APM. The APM will remain stable when the tip is retracted or when the current is switched off.

A perceptive reader may also notice some vague step like features in the frequency–current graph (figure 4(B)), which are superimposed on the overall linear trend. Despite some scatter in the data points it seems unlikely that the steps are experimental artifacts. Each data point in this graph is by itself an average over at least 500 flipping events. If the steps are real, then it means that within each step plateau the APM tries to keep its average flipping frequency constant regardless of a variation in the tunneling current. In addition, reexamination of figure 4(A) indeed reveals that the change of the flipping frequency with varying tunneling current becomes rather abrupt around $t = 50$ s. Since there is no sudden change in the tunneling current at $t = 50$ s, the only explanation is that the APM undergoes an electronic rearrangement, which is independent of the structural configuration of the APM and only depends on the tip–APM distance. One possible explanation might be that the APM—or something in its vicinity—behaves as a small quantum dot (QD). Adding (subtracting) an extra electron to (from) the QD changes the electronic structure of the APM abruptly. The latter might for instance lead to different excitation efficiencies for the incoming or outgoing tunneling electrons. It is well known from the orthodox theory of Coulomb blockade that, at a constant bias voltage, the charge accumulated on the QD depends on the capacitances and resistances of its two tunnel

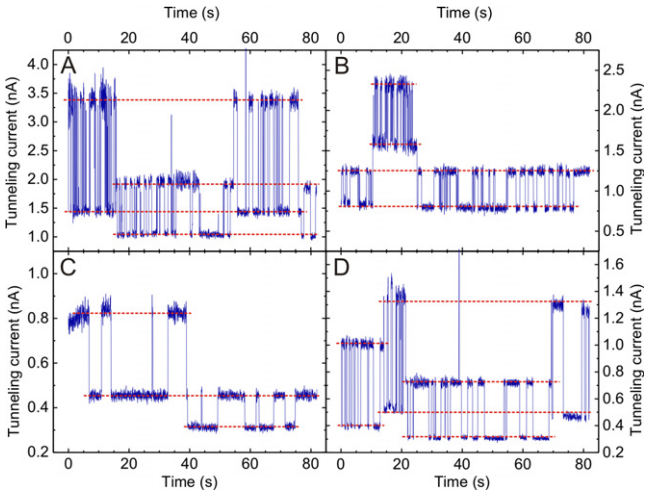

Figure 5. Transitions of the APM between different flipping modes at 77 K, gap voltage −1.0 V, open feedback loop and initial tunneling currents of 1.5, 0.8, 0.8 and 1.0 nA for (A)–(D). (A) The APM exhibits three back and forth transitions between two distinct flipping modes. (B) Current time trace of a four level system. (C) Transition of the APM between two flipping modes where one of the configurations is common to both modes. (D) The APM exhibits several transitions between three distinct flipping modes, revealing that the APM can reside in six well-defined states.

junctions. By changing the tip–APM distance, the capacitance and resistance of the tip–QD junction changes continuously. This leads to quantized changes of the charge on the QD. Since each APM flipping event is induced by an inelastic tunneling electron, this can explain the stepwise decrease of the flipping frequency. To study this tentative model in more detail we have plotted the residence time distribution of the LC and HC states separately in figure 4(C). Surprisingly the residence time distribution lines of LC and HC states collapse onto each other. If our last assumption—that each APM flipping event is caused by an inelastic electron that tunnels to the QD—is true, then this implies that the QD receives or emits about the same amount of electrons in the HC and LC states. The latter requires that the QD character of the APM remains stationary upon flipping back and forth, so we have to exclude the revolving atoms of the APM being part of the QD. Hence either the pivot atoms or some subsurface impurity, i.e. for instance a dopant atom, might act as the QD. What remains puzzling in this tentative model is the coupling of the QD with the substrate. It is by no means clear why there should be a tunneling barrier between the embedded QD and the surrounding substrate.

Figure 5 shows more current–time traces revealing that the dynamic behavior of the APM is more complex than just a simple two level system. All depicted current time traces are corrected for drift. Figure 5(A) shows that the APM can reside in at least four states. At each stage, the APM is flipping black and forth between two well-defined states. Figure 5(B) again shows the APM flipping between four states, however, the flipping modes are different from the ones shown in figure 5(A). Figure 5(C) shows the APM changing its flipping mode around $t = 40$ s, but the new flipping mode shares a state with the previous one. Even more interesting is figure 5(D), which reveals that the APM can reside in not less than six distinct states. To understand how the APM can reside in six states while having only two moving components it is necessary to develop a model. Figure 6(A) shows the four possible configurations of the APM dimer pair. These four configurations define a total of four current levels. The fact that the two revolving atoms of the APM dimers are able to flip back and forth, implies that they are only weakly bounded to the underlying Ge(001) substrate. The two purple circles in figure 6 refer to atoms of the underlying substrate (see figures 1(B) and (E)). It might be that these substrate atoms provide the bonding that is needed to, at least temporarily, lock the APM in one of its stable configurations. Using the four states or current levels, one can define six possible telegraphic signals, as is schematically depicted in figure 6(B). We propose that there are two additional current levels, due to the fact that in flipping mode 6 the revolving atoms do not reach their maximum amplitude. An attractive interaction between the two revolving atoms not only explains this reduced amplitude of flipping mode 6, but it also accounts for the absence of the out-of-phase flipping mode number 5. By comparing the experimental current–time traces with the model, one can easily understand the rich dynamics of the APM. For instance, figure 5(A) shows that the APM changes its mode from flipping mode 1 to 2, to 1, and finally back to flipping mode 2. In

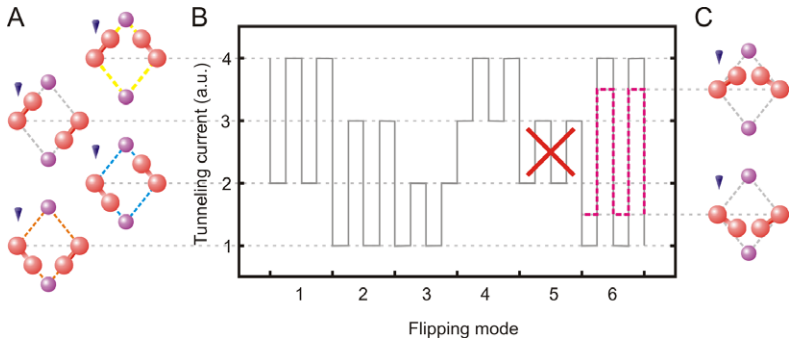

Figure 6. (A) A ball model of the APM showing the four possible configurations. The flipping dimers are represented by dumbbells and the two circles above and below the dumbbells are reference atoms of the underlying terrace (see the arrows in figure 3(B)). (B) For the tip position, outlined in panel (A) by the small cone, four current levels and six different flipping modes are found. (C) By including an attractive interaction between the revolving atoms, flipping mode 5 will not occur and the amplitude of flipping mode 6 is somewhat smaller.

figure 5(B) the only possible option is flipping from mode 3 to 4 and then back to flipping mode 3. For figure 5(C) we have two options: mode 1 to mode 3, or mode 4 to mode 2. And finally for figure 5(D), the only option is the sequence mode 6–1–2–6.

5. Conclusions

Dynamical processes on surfaces can show up in conventional STM images as discontinuities or distortions in the appearance of atoms. In order to study these dynamic processes one has to improve the time resolution significantly. A versatile way to do this with a conventional STM is to record current–time traces with the feedback loop switched off. One should, however, realize that the drastically improved time resolution comes at the expense of the ability to obtain spatial information. In this article we provide two examples of this technique. In the first example the dynamics of adatoms of a Ge(111)-c(2 × 8) surface is studied, whereas in the second example we have analyzed the complex dynamics of a dimer pair of the Pt modified Ge(001) surface.

Acknowledgment

Authors would like to acknowledge the financial support of Nanoned for this project (STW Project number: TTF.6947).

References

[1] Müller E W 1951 *Z. Phys.* **131** 136
[2] Binnig G and Rohrer H 1982 *Helv. Phys. Acta* **5** 726
[3] Ganz E, Theiss S K, Hwang I S and Golovchenko K 1992 *Phys. Rev. Lett.* **68** 1567
[4] Zandvliet H J W, Galea T M, Zoethout E and Poelsema B 2000 *Phys. Rev. Lett.* **84** 1523
[5] Zandvliet H J W, Elswijk H B and van Loenen E J 1992 *Surf. Sci.* **272** 264
[6] Li J T, Berndt R and Schneider W D 1996 *Phys. Rev. Lett.* **76** 1888
[7] Besenbacher F, Laegsgaard E and Stensgaard I 2005 *Mater. Today* **8** 26
[8] Rost M J, Carma L, Schakel P, van Tol E, van Velzen-Williams G B E M, Overgauw C F, ter Horst H, Dekker H, Okhuijsen B, Seynen M, Vijftigschild A, Han P, Katan A J, Schoots K, Schumm R, van Loo W, Oosterkamp T H and Frenken J W M 2005 *Rev. Sci. Instrum.* **76** 053710
[9] Becker R S, Golovchenko J A and Swartzentruber B S 1985 *Phys. Rev. Lett.* **54** 2678
[10] Becker R S, Swartzentruber B S, Vickers J S and Klitsner T 1989 *Phys. Rev.* B **39** 1633
[11] Phaneuf R J and Webb M B 1985 *Surf. Sci.* **164** 167
[12] Zandvliet H J W and van Silfhout A 1988 *Surf. Sci.* **195** 138
[13] Takeuchi N, Selloni A and Tosatti E 1992 *Phys. Rev. Lett.* **69** 648
[14] Takeuchi N, Selloni A and Tosatti E 1994 *Surf. Sci.* **307** 755
[15] Meade R D and Vanderbilt D 1989 *Phys. Rev.* B **40** 3905
[16] Feenstra R M, Gaan S, Meyer G and Rieder K H 2005 *Phys. Rev.* B **71** 125316
[17] Feenstra R M, Lee J Y, Kang M H, Meyer G and Rieder K H 2006 *Phys. Rev.* B **73** 035310
[18] Feenstra R M and Slavin A J 1991 *Surf. Sci.* **251/252** 401
[19] Gai Z, Yu H and Wang W S 1996 *Phys. Rev.* B **53** 13547
[20] Kaxiras A and Erlebacher J 1994 *Phys. Rev. Lett.* **72** 1714
[21] Hwang I S and Golovchenko J 1992 *Science* **258** 1119
[22] Zandvliet H J W 2003 *Phys. Rep.* **388** 1
[23] Sato T, Iwatsuki M and Tochihara H 1999 *J. Electron Microsc.* **48** 1
[24] van Houselt A, van Gastel R, Poelsema B and Zandvliet H J W 2006 *Phys. Rev. Lett.* **97** 266104
[25] Gurlu O, Adam O A O, Zandvliet H J W and Poelsema B 2003 *Appl. Phys. Lett.* **83** 4610
[26] Oncel N, van Houselt A, Huijben J, Hallbäck A S, Gurlu O, Zandvliet H J W and Poelsema B 2005 *Phys. Rev. Lett.* **95** 116801
[27] van Houselt A, Gnielka T, Fischer M, Aan de Brugh J M J, Oncel N, Kockmann D, Heid R, Bohnen K P, Poelsema B and Zandvliet H J W 2008 *Surf. Sci.* **602** 1731
[28] Saedi A, van Houselt A, van Gastel R, Poelsema B and Zandvliet H J W 2009 *Nano Lett.* **9** 1733